EUROPEAN ORGANIZATION FOR NUCLEAR RESEARCH

CERN–PPE/96–185

12 December 1996

A Measurement of α_s from the Scaling Violation in e^+e^- Annihilation

DELPHI Collaboration

Abstract

The hadronic fragmentation functions of the various quark flavours and of gluons are measured in a study of the inclusive hadron production from Z^0 decays with the DELPHI detector and are compared with the fragmentation functions measured elsewhere at energies between 14 GeV and 91 GeV. A large scaling violation is observed, which is used to extract the strong coupling constant from a fit using a numerical integration of the second order DGLAP evolution equations. The result is

$$\alpha_s(M_Z) = 0.124^{+0.006}_{-0.007}(exp) \pm 0.009(theory)$$

where the first error represents the experimental uncertainty and the second error is due to the factorization and renormalization scale dependence.

(To be submitted to Physics Letters B)

P.Abreu[21], W.Adam[50], T.Adye[37], I.Ajinenko[42], G.D.Alekseev[16], R.Alemany[49], P.P.Allport[22], S.Almehed[24], U.Amaldi[9], S.Amato[47], A.Andreazza[28], M.L.Andrieux[14], P.Antilogus[9], W-D.Apel[17], B.Åsman[44], J-E.Augustin[25], A.Augustinus[9], P.Baillon[9], P.Bambade[19], F.Barao[21], M.Barbi[47], G.Barbiellini[46], D.Y.Bardin[16], G.Barker[9], A.Baroncelli[40], O.Barring[24], J.A.Barrio[26], W.Bartl[50], M.J.Bates[37], M.Battaglia[15], M.Baubillier[23], J.Baudot[39], K-H.Becks[52], M.Begalli[6], P.Beilliere[8], Yu.Belokopytov[9,53], A.C.Benvenuti[5], M.Berggren[47], D.Bertini[25], D.Bertrand[2], M.Besancon[39], F.Bianchi[45], M.Bigi[45], M.S.Bilenky[16], P.Billoir[23], M-A.Bizouard[19], D.Bloch[10], M.Blume[52], T.Bolognese[39], M.Bonesini[28], W.Bonivento[28], P.S.L.Booth[22], C.Bosio[40], O.Botner[48], E.Boudinov[31], B.Bouquet[19], C.Bourdarios[9], T.J.V.Bowcock[22], M.Bozzo[13], P.Branchini[40], K.D.Brand[36], T.Brenke[52], R.A.Brenner[15], C.Bricman[2], R.C.A.Brown[9], P.Bruckman[18], J-M.Brunet[8], L.Bugge[33], T.Buran[33], T.Burgsmueller[52], P.Buschmann[52], S.Cabrera[49], M.Caccia[28], M.Calvi[28], A.J.Camacho Rozas[41], T.Camporesi[9], V.Canale[38], M.Canepa[13], K.Cankocak[44], F.Cao[2], F.Carena[9], L.Carroll[22], C.Caso[13], M.V.Castillo Gimenez[49], A.Cattai[9], F.R.Cavallo[5], V.Chabaud[9], Ph.Charpentier[9], L.Chaussard[25], P.Checchia[36], G.A.Chelkov[16], M.Chen[2], R.Chierici[45], P.Chliapnikov[42], P.Chochula[7], V.Chorowicz[9], J.Chudoba[30], V.Cindro[43], P.Collins[9], R.Contri[13], E.Cortina[49], G.Cosme[19], F.Cossutti[46], J-H.Cowell[22], H.B.Crawley[1], D.Crennell[37], G.Crosetti[13], J.Cuevas Maestro[34], S.Czellar[15], E.Dahl-Jensen[29], J.Dahm[52], B.Dalmagne[19], M.Dam[29], G.Damgaard[29], P.D.Dauncey[37], M.Davenport[9], W.Da Silva[23], C.Defoix[8], A.Deghorain[2], G.Della Ricca[46], P.Delpierre[27], N.Demaria[35], A.De Angelis[9], W.De Boer[17], S.De Brabandere[2], C.De Clercq[2], C.De La Vaissiere[23], B.De Lotto[46], A.De Min[36], L.De Paula[47], C.De Saint-Jean[39], H.Dijkstra[9], L.Di Ciaccio[38], A.Di Diodato[38], F.Djama[10], A.Djannati[8], J.Dolbeau[8], K.Doroba[51], M.Dracos[10], J.Drees[52], K.-A.Drees[52], M.Dris[32], J-D.Durand[25,9], D.Edsall[1], R.Ehret[17], G.Eigen[4], T.Ekelof[48], G.Ekspong[44], M.Elsing[9], J-P.Engel[10], B.Erzen[43], M.Espirito Santo[21], E.Falk[24], D.Fassouliotis[32], M.Feindt[9], A.Fenyuk[42], A.Ferrer[49], S.Fichet[23], T.A.Filippas[32], A.Firestone[1], P.-A.Fischer[10], H.Foeth[9], E.Fokitis[32], F.Fontanelli[13], F.Formenti[9], B.Franek[37], P.Frenkiel[8], D.C.Fries[17], A.G.Frodesen[4], R.Fruhwirth[50], F.Fulda-Quenzer[19], J.Fuster[49], A.Galloni[22], D.Gamba[45], M.Gandelman[47], C.Garcia[49], J.Garcia[41], C.Gaspar[9], U.Gasparini[36], Ph.Gavillet[9], E.N.Gazis[32], D.Gele[10], J-P.Gerber[10], L.Gerdyukov[42], R.Gokieli[51], B.Golob[43], G.Gopal[37], L.Gorn[1], M.Gorski[51], Yu.Gouz[45,53], V.Gracco[13], E.Graziani[40], C.Green[22], A.Grefrath[52], P.Gris[39], G.Grosdidier[19], K.Grzelak[51], S.Gumenyuk[28,53], P.Gunnarsson[44], M.Gunther[48], J.Guy[37], F.Hahn[9], S.Hahn[52], Z.Hajduk[18], A.Hallgren[48], K.Hamacher[52], F.J.Harris[35], V.Hedberg[24], R.Henriques[21], J.J.Hernandez[49], P.Herquet[2], H.Herr[9], T.L.Hessing[35], J.-M.Heuser[52], E.Higon[49], H.J.Hilke[9], T.S.Hill[1], S-O.Holmgren[44], P.J.Holt[35], D.Holthuizen[31], S.Hoorelbeke[2], M.Houlden[22], J.Hrubec[50], K.Huet[2], K.Hultqvist[44], J.N.Jackson[22], R.Jacobsson[44], P.Jalocha[18], R.Janik[7], Ch.Jarlskog[24], G.Jarlskog[24], P.Jarry[39], B.Jean-Marie[19], E.K.Johansson[44], L.Jonsson[24], P.Jonsson[24], C.Joram[9], P.Juillot[10], M.Kaiser[17], F.Kapusta[23], K.Karafasoulis[11], M.Karlsson[44], E.Karvelas[11], S.Katsanevas[3], E.C.Katsoufis[32], R.Keranen[4], Yu.Khokhlov[42], B.A.Khomenko[16], N.N.Khovanski[16], B.King[22], N.J.Kjaer[31], O.Klapp[52], H.Klein[9], A.Klovning[4], P.Kluit[31], B.Koene[31], P.Kokkinias[11], M.Koratzinos[9], K.Korcyl[18], V.Kostioukhine[42], C.Kourkoumelis[3], O.Kouznetsov[13,16], M.Krammer[50], C.Kreuter[9], I.Kronkvist[24], Z.Krumstein[16], W.Krupinski[18], P.Kubinec[7], W.Kucewicz[18], K.Kurvinen[15], C.Lacasta[49], I.Laktineh[25], J.W.Lamsa[1], L.Lanceri[46], D.W.Lane[1], P.Langefeld[52], V.Lapin[42], J-P.Laugier[39], R.Lauhakangas[15], G.Leder[50], F.Ledroit[14], V.Lefebure[2], C.K.Legan[1], R.Leitner[30], J.Lemonne[2], G.Lenzen[52], V.Lepeltier[19], T.Lesiak[18], J.Libby[35], D.Liko[9], R.Lindner[52], A.Lipniacka[44], I.Lippi[36], B.Loerstad[24], J.G.Loken[35], J.M.Lopez[41], D.Loukas[11], P.Lutz[39], L.Lyons[35], J.MacNaughton[50], G.Maehlum[17], J.R.Mahon[6], A.Maio[21], T.G.M.Malmgren[44], V.Malychev[16], F.Mandl[50], J.Marco[41], R.Marco[41], B.Marechal[47], M.Margoni[36], J-C.Marin[9], C.Mariotti[9], A.Markou[11], C.Martinez-Rivero[34], F.Martinez-Vidal[49], S.Marti i Garcia[22], J.Masik[30], F.Matorras[41], C.Matteuzzi[28], G.Matthiae[38], M.Mazzucato[36], M.Mc Cubbin[22], R.Mc Kay[1], R.Mc Nulty[22], J.Medbo[48], M.Merk[31], C.Meroni[28], S.Meyer[17], W.T.Meyer[1], A.Miagkov[42], M.Michelotto[36], E.Migliore[45], L.Mirabito[25], W.A.Mitaroff[50], U.Mjoernmark[24], T.Moa[44], R.Moeller[29], K.Moenig[9], M.R.Monge[13], P.Morettini[13], H.Mueller[17], K.Muenich[52], M.Mulders[31], L.M.Mundim[6], W.J.Murray[37], B.Muryn[14,18], G.Myatt[35], F.Naraghi[14], F.L.Navarria[5], S.Navas[49], K.Nawrocki[51], P.Negri[28], W.Neumann[52], N.Neumeister[50], R.Nicolaidou[3], B.S.Nielsen[29], M.Nieuwenhuizen[31], V.Nikolaenko[10], P.Niss[44], A.Nomerotski[36], A.Normand[35], W.Oberschulte-Beckmann[17], V.Obraztsov[42], A.G.Olshevski[16], R.Orava[15], G.Orazi[10], K.Osterberg[15], A.Ouraou[39], P.Paganini[19], M.Paganoni[9,28], P.Pages[10], R.Pain[23], H.Palka[18], Th.D.Papadopoulou[32], K.Papageorgiou[11], L.Pape[9], C.Parkes[35], F.Parodi[13], A.Passeri[40], M.Pegoraro[36], L.Peralta[21], H.Pernegger[50], M.Pernicka[50], A.Perrotta[5], C.Petridou[46], A.Petrolini[13], M.Petrovyck[42], H.T.Phillips[37], G.Piana[13], F.Pierre[39], M.Pimenta[21], T.Podobnik[43], O.Podobrin[9], M.E.Pol[6], G.Polok[18], P.Poropat[46], V.Pozdniakov[16], P.Privitera[38], N.Pukhaeva[16], A.Pullia[28], D.Radojicic[35], S.Ragazzi[28], H.Rahmani[32], J.Rames[12], P.N.Ratoff[20], A.L.Read[33], M.Reale[52], P.Rebecchi[19], N.G.Redaelli[28], D.Reid[9], R.Reinhardt[52], P.B.Renton[35], L.K.Resvanis[3], F.Richard[19], J.Richardson[22], J.Ridky[12], G.Rinaudo[45], I.Ripp[39], A.Romero[45], I.Roncagliolo[13], P.Ronchese[36], L.Roos[23], E.I.Rosenberg[1], P.Roudeau[19], T.Rovelli[5], W.Ruckstuhl[31], V.Ruhlmann-Kleider[39], A.Ruiz[41], K.Rybicki[18], H.Saarikko[15], Y.Sacquin[39], A.Sadovsky[16], O.Sahr[14], G.Sajot[14], J.Salt[49], J.Sanchez[26], M.Sannino[13], M.Schimmelpfennig[17], H.Schneider[17], U.Schwickerath[17], M.A.E.Schyns[52], G.Sciolla[45], F.Scuri[46], P.Seager[20], Y.Sedykh[16], A.M.Segar[35], A.Seitz[17], R.Sekulin[37], L.Serbelloni[38], R.C.Shellard[6], P.Siegrist[39], R.Silvestre[39], S.Simonetti[39], F.Simonetto[36], A.N.Sisakian[16], B.Sitar[7], T.B.Skaali[33], G.Smadja[25], N.Smirnov[42], O.Smirnova[24], G.R.Smith[37], R.Sosnowski[51], D.Souza-Santos[6], T.Spassov[21], E.Spiriti[40], P.Sponholz[52], S.Squarcia[13], D.Stampfer[9], C.Stanescu[40], S.Stanic[43], S.Stapnes[33], I.Stavitski[36], K.Stevenson[35], A.Stocchi[19], J.Strauss[50],

R.Strub[10], B.Stugu[4], M.Szczekowski[51], M.Szeptycka[51], T.Tabarelli[28], J.P.Tavernet[23], O.Tchikilev[42], J.Thomas[35], A.Tilquin[27], J.Timmermans[31], L.G.Tkatchev[16], T.Todorov[10], S.Todorova[10], D.Z.Toet[31], A.Tomaradze[2], B.Tome[21], A.Tonazzo[28], L.Tortora[40], G.Transtromer[24], D.Treille[9], G.Tristram[8], A.Trombini[19], C.Troncon[28], A.Tsirou[9], M-L.Turluer[39], I.A.Tyapkin[16], M.Tyndel[37], S.Tzamarias[22], B.Ueberschaer[52], O.Ullaland[9], V.Uvarov[42], G.Valenti[5], E.Vallazza[9], G.W.Van Apeldoorn[31], P.Van Dam[31], J.Van Eldik[31], A.Van Lysebetten[2], N.Vassilopoulos[35], G.Vegni[28], L.Ventura[36], W.Venus[37], F.Verbeure[2], M.Verlato[36], L.S.Vertogradov[16], D.Vilanova[39], P.Vincent[25], L.Vitale[46], E.Vlasov[42], A.S.Vodopyanov[16], V.Vrba[12], H.Wahlen[52], C.Walck[44], M.Weierstall[52], P.Weilhammer[9], C.Weiser[17], A.M.Wetherell[9], D.Wicke[52], J.H.Wickens[2], M.Wielers[17], G.R.Wilkinson[9], W.S.C.Williams[35], M.Winter[10], M.Witek[18], T.Wlodek[19], K.Woschnagg[48], K.Yip[35], O.Yushchenko[42], F.Zach[25], A.Zaitsev[42], A.Zalewska[9], P.Zalewski[51], D.Zavrtanik[43], E.Zevgolatakos[11], N.I.Zimin[16], M.Zito[39], D.Zontar[43], G.C.Zucchelli[44], G.Zumerle[36]

[1] Department of Physics and Astronomy, Iowa State University, Ames IA 50011-3160, USA
[2] Physics Department, Univ. Instelling Antwerpen, Universiteitsplein 1, B-2610 Wilrijk, Belgium
and IIHE, ULB-VUB, Pleinlaan 2, B-1050 Brussels, Belgium
and Faculté des Sciences, Univ. de l'Etat Mons, Av. Maistriau 19, B-7000 Mons, Belgium
[3] Physics Laboratory, University of Athens, Solonos Str. 104, GR-10680 Athens, Greece
[4] Department of Physics, University of Bergen, Allégaten 55, N-5007 Bergen, Norway
[5] Dipartimento di Fisica, Università di Bologna and INFN, Via Irnerio 46, I-40126 Bologna, Italy
[6] Centro Brasileiro de Pesquisas Físicas, rua Xavier Sigaud 150, RJ-22290 Rio de Janeiro, Brazil
and Depto. de Física, Pont. Univ. Católica, C.P. 38071 RJ-22453 Rio de Janeiro, Brazil
and Inst. de Física, Univ. Estadual do Rio de Janeiro, rua São Francisco Xavier 524, Rio de Janeiro, Brazil
[7] Comenius University, Faculty of Mathematics and Physics, Mlynska Dolina, SK-84215 Bratislava, Slovakia
[8] Collège de France, Lab. de Physique Corpusculaire, IN2P3-CNRS, F-75231 Paris Cedex 05, France
[9] CERN, CH-1211 Geneva 23, Switzerland
[10] Centre de Recherche Nucléaire, IN2P3 - CNRS/ULP - BP20, F-67037 Strasbourg Cedex, France
[11] Institute of Nuclear Physics, N.C.S.R. Demokritos, P.O. Box 60228, GR-15310 Athens, Greece
[12] FZU, Inst. of Physics of the C.A.S. High Energy Physics Division, Na Slovance 2, 180 40, Praha 8, Czech Republic
[13] Dipartimento di Fisica, Università di Genova and INFN, Via Dodecaneso 33, I-16146 Genova, Italy
[14] Institut des Sciences Nucléaires, IN2P3-CNRS, Université de Grenoble 1, F-38026 Grenoble Cedex, France
[15] Research Institute for High Energy Physics, SEFT, P.O. Box 9, FIN-00014 Helsinki, Finland
[16] Joint Institute for Nuclear Research, Dubna, Head Post Office, P.O. Box 79, 101 000 Moscow, Russian Federation
[17] Institut für Experimentelle Kernphysik, Universität Karlsruhe, Postfach 6980, D-76128 Karlsruhe, Germany
[18] Institute of Nuclear Physics and University of Mining and Metalurgy, Ul. Kawiory 26a, PL-30055 Krakow, Poland
[19] Université de Paris-Sud, Lab. de l'Accélérateur Linéaire, IN2P3-CNRS, Bât. 200, F-91405 Orsay Cedex, France
[20] School of Physics and Chemistry, University of Lancaster, Lancaster LA1 4YB, UK
[21] LIP, IST, FCUL - Av. Elias Garcia, 14-1°, P-1000 Lisboa Codex, Portugal
[22] Department of Physics, University of Liverpool, P.O. Box 147, Liverpool L69 3BX, UK
[23] LPNHE, IN2P3-CNRS, Universités Paris VI et VII, Tour 33 (RdC), 4 place Jussieu, F-75252 Paris Cedex 05, France
[24] Department of Physics, University of Lund, Sölvegatan 14, S-22363 Lund, Sweden
[25] Université Claude Bernard de Lyon, IPNL, IN2P3-CNRS, F-69622 Villeurbanne Cedex, France
[26] Universidad Complutense, Avda. Complutense s/n, E-28040 Madrid, Spain
[27] Univ. d'Aix - Marseille II - CPP, IN2P3-CNRS, F-13288 Marseille Cedex 09, France
[28] Dipartimento di Fisica, Università di Milano and INFN, Via Celoria 16, I-20133 Milan, Italy
[29] Niels Bohr Institute, Blegdamsvej 17, DK-2100 Copenhagen 0, Denmark
[30] NC, Nuclear Centre of MFF, Charles University, Areal MFF, V Holesovickach 2, 180 00, Praha 8, Czech Republic
[31] NIKHEF, Postbus 41882, NL-1009 DB Amsterdam, The Netherlands
[32] National Technical University, Physics Department, Zografou Campus, GR-15773 Athens, Greece
[33] Physics Department, University of Oslo, Blindern, N-1000 Oslo 3, Norway
[34] Dpto. Fisica, Univ. Oviedo, Avda. Calvo Sotelo, S/N-33007 Oviedo, Spain, (CICYT-AEN96-1681)
[35] Department of Physics, University of Oxford, Keble Road, Oxford OX1 3RH, UK
[36] Dipartimento di Fisica, Università di Padova and INFN, Via Marzolo 8, I-35131 Padua, Italy
[37] Rutherford Appleton Laboratory, Chilton, Didcot OX11 OQX, UK
[38] Dipartimento di Fisica, Università di Roma II and INFN, Tor Vergata, I-00173 Rome, Italy
[39] CEA, DAPNIA/Service de Physique des Particules, CE-Saclay, F-91191 Gif-sur-Yvette Cedex, France
[40] Istituto Superiore di Sanità, Ist. Naz. di Fisica Nucl. (INFN), Viale Regina Elena 299, I-00161 Rome, Italy
[41] Instituto de Fisica de Cantabria (CSIC-UC), Avda. los Castros, S/N-39006 Santander, Spain, (CICYT-AEN96-1681)
[42] Inst. for High Energy Physics, Serpukov P.O. Box 35, Protvino, (Moscow Region), Russian Federation
[43] Department of Astroparticle Physics, School of Environmental Sciences, Nova Gorica, and J. Stefan Institute, Ljubljana, Slovenia
[44] Fysikum, Stockholm University, Box 6730, S-113 85 Stockholm, Sweden
[45] Dipartimento di Fisica Sperimentale, Università di Torino and INFN, Via P. Giuria 1, I-10125 Turin, Italy
[46] Dipartimento di Fisica, Università di Trieste and INFN, Via A. Valerio 2, I-34127 Trieste, Italy
and Istituto di Fisica, Università di Udine, I-33100 Udine, Italy
[47] Univ. Federal do Rio de Janeiro, C.P. 68528 Cidade Univ., Ilha do Fundão BR-21945-970 Rio de Janeiro, Brazil
[48] Department of Radiation Sciences, University of Uppsala, P.O. Box 535, S-751 21 Uppsala, Sweden
[49] IFIC, Valencia-CSIC, and D.F.A.M.N., U. de Valencia, Avda. Dr. Moliner 50, E-46100 Burjassot (Valencia), Spain
[50] Institut für Hochenergiephysik, Österr. Akad. d. Wissensch., Nikolsdorfergasse 18, A-1050 Vienna, Austria
[51] Inst. Nuclear Studies and University of Warsaw, Ul. Hoza 69, PL-00681 Warsaw, Poland
[52] Fachbereich Physik, University of Wuppertal, Postfach 100 127, D-42097 Wuppertal, Germany
[53] On leave of absence from IHEP Serpukhov

1 Introduction

Hadron production in e^+e^- annihilation originates from the production of quark-antiquark pairs which can radiate gluons, the quanta of the field theory of the strong interactions, Quantum ChromoDynamics (QCD). Gluon radiation depends logarithmically on the centre of mass energy Q, due to the increase in phase space with increasing energy and to the energy dependence of the running coupling constant of QCD, $\alpha_s(Q)$. These effects lead to logarithmic dependences of the momentum spectra of the produced hadrons on the centre of mass energy, even if the momenta are scaled to that energy. These scaling violations can be used to determine the strong coupling constant α_s.

Our previous analysis of this type [1] was based on the exact second order matrix-element and string or independent fragmentation, with a relatively small number of free parameters. A precise measurement was obtained, $\alpha_s(M_Z) = 0.118 \pm 0.005$, in agreement with α_s measurements at the Z^0 mass from shape variables, from jet rates and from total cross-sections, measured at the electron-positron storage ring LEP [2–4].

This paper extends that analysis by including new data on gluon and heavy quark fragmentation and using a numerical integration of the second order DGLAP evolution equations [5], employing the program of Nason and Webber [6]. This approach uses a summation of the leading logarithms, in contrast to our previous analysis which used a numerical Monte Carlo integration over the complete second order matrix element. Additional differences between the two analyses are as follows.

1. In the DGLAP equations, the higher orders are resummed for soft and collinear gluons, while the hard gluons are calculated only in first order. In the previous analysis using the QCD matrix element, all gluons were calculated up to exact second order without a resummation of the leading logarithmic terms.
2. The separation between the perturbative and non-perturbative regime is handled differently: with the matrix element, the separation is done by a cut on invariant masses between quark and gluons, while in the DGLAP approach the factorization theorem states that the two regimes can be separated at an arbitrary factorization scale.

Thus this measurement provides a useful cross check of the previous result with different systematics.

The DGLAP equations are based on the concept of independent quark and gluon fragmentation since each parton fragments according to a particular parametrization, independently of the other partons. In contrast, the QCD predictions were based on the fragmentation of colour flux tubes stretched between the partons. However, in our previous analysis [1], we showed that both independent and string fragmentation models led to the same results. This is not surprising, since α_s is determined from the differences between the parametrizations of the momentum spectra at different energies, so many systematic uncertainties cancel.

2 Phenomenology of inclusive hadroproduction

The inclusive production of charged hadrons in the reaction $e^+e^- \to h^\pm + X$ can be described by two kinematic variables, Q^2 and x, where Q^2 is defined as the square of the four-momentum transferred from the leptons to the hadrons and $x = p_h/p_{beam}$ is the fraction of the beam momentum p_{beam} carried by the hadron h. In e^+e^- annihilation, Q^2 equals s, the total centre-of-mass energy squared.

The total cross-section for $e^+e^- \to h^\pm + X$ can be factorized into two regimes: the short distance regime, in which hard gluons can be radiated, and the long distance regime of the hadronization process. The short distance regime is calculable perturbatively in terms of the so-called coefficient functions, while the non-calculable long distance regime has to be parametrized by phenomenological fragmentation functions. Combining the two regimes according to the factorization theorem yields the following expression for the cross-section [6]:

$$\frac{d\sigma}{dx}(e^+e^- \longrightarrow h + X) \;=\; \sum_i \int_x^1 \frac{dz}{z}\; C_i\{z, \alpha_s(\mu_R), \mu_F^2/Q^2\}\; D_i\{\frac{x}{z}, \mu_F^2\} \qquad (1)$$

where the C_i are the coefficient functions for the creation of a parton with flavour i and momentum fraction $z = p_{parton}/p_{beam}$, while the fragmentation functions D_i represent the probability that parton i fragments into the hadron h with momentum fraction x/z. In leading order, the C_i are given by the flavour specific weights of the electroweak theory, and the α_s dependence of the C_i represents the next-to-leading order QCD corrections to the primary quark-pair production. Both the coefficient and fragmentation functions depend on an arbitrary factorization scale μ_F, in such a way that the dependence of the physical cross-section on μ_F would cancel if the calculation could be carried out to all orders in perturbation theory. In principle, the renormalization scale μ_R used for α_s in (1) could be chosen differently from the factorization scale μ_F; for simplicity, the two scales have been taken to be the same. The sum runs over all possible partons: u, d, c, s, b, g.

The scaling violation in the fragmentation function is described by coupled integro-differential evolution equations [5], which can be written as:

$$\frac{dD_j(x,Q^2)}{d\ln Q^2} = \sum_i \int_x^1 \frac{dz}{z} P_{ij}\{z, \alpha_s(\mu_R), \frac{\mu_R^2}{Q^2}\}\; D_i\{\frac{x}{z}, Q^2\} \qquad (2)$$

with the splitting functions

$$P_{ij}\{z, \alpha_s(\mu_R), \frac{\mu_R^2}{Q^2}\} = \frac{\alpha_s(\mu_R)}{2\pi}\; P_{ij}^{(0)}(z) + \left(\frac{\alpha_s(\mu_R)}{2\pi}\right)^2 P_{ij}^{(1)}\{z, \frac{\mu_R^2}{Q^2}\} + O(\alpha_s^3).$$

The indices i and j run over all active quarks, antiquarks and the gluon. The splitting functions $P_{ij}(z)$ are the probabilities for finding parton i with momentum fraction z after splitting from its parent parton j. The $P_{ij}(z)$ are known to next-to-leading order in perturbation theory [7]. Thus the fragmentation functions at a given energy Q_0 can be fitted to experimental data using equation (1), and then evolved to a different energy using the evolution equations (2). The strong coupling constant can then be extracted from a simultaneous fit of these calculated spectra to the data at different centre-of-mass energies.

The strong coupling constant, α_s, depends on the energy or scale, μ_R. Since we compare momentum spectra at different energies, it is more convenient to fit the energy independent QCD scale $\Lambda^{(5)}_{\overline{MS}}$ (for 5 flavours in the $\overline{MS}$ renormalization scheme), which is related to α_s at the scale μ by

$$\begin{aligned}\alpha_s(\mu) \;&=\; \frac{4\pi}{\beta_0 \ln(\mu/\Lambda^{(5)}_{\overline{MS}})^2}\left[1 - 2\frac{\beta_1}{\beta_0^2}\frac{\ln[\ln(\mu/\Lambda^{(5)}_{\overline{MS}})^2]}{\ln(\mu/\Lambda^{(5)}_{\overline{MS}})^2}\right.\\ &+\; \left.\frac{4\beta_1^2}{\beta_0^4 \ln^2(\mu/\Lambda^{(5)}_{\overline{MS}})^2}\left(\left(\ln[\ln(\mu/\Lambda^{(5)}_{\overline{MS}})^2] - \frac{1}{2}\right)^2 + \frac{\beta_2\beta_0}{8\beta_1^2} - \frac{5}{4}\right)\right] \qquad (3)\end{aligned}$$

with $\beta_0 = 11 - \frac{2}{3}N_f$, $\beta_1 = 51 - \frac{19}{3}N_f$, and $\beta_2 = 2857 - \frac{5033}{9}N_f - \frac{325}{27}N_f^2$, where $N_f = 5$ is the number of quark flavours [8].

3 Measurements of inclusive hadron distributions

This analysis uses 1.75 million hadronic Z^0 decays collected with the DELPHI detector [9] in the years 1991 to 1993.

Samples enriched in bottom (b), charm (c), and light (uds) quarks were used to determine the scaled momentum distributions $1/\sigma\, d\sigma/dx$ for each quark flavour separately. In addition, the scaled momentum distribution for charged particles from gluon fragmentation was obtained from 3-jet events.

These distributions define the fragmentation functions averaged over all final state hadrons and can be obtained from the total number of events N_{tot} and the number of charged particles for each x bin $N^{(i)}$:

$$D_i(x,Q^2) \equiv \frac{1}{\sigma_i}\frac{d\sigma_i}{dx} = \frac{1}{N_{tot}}\frac{dN^{(i)}}{dx}. \tag{4}$$

Hadronic events were selected by requiring at least 5 charged particles with momenta above 0.2 GeV/c and track lengths in the detector of at least 50 cm, a total energy of the charged particles exceeding 15 GeV (assuming pion masses) including at least 3 GeV in both the forward and the backward hemisphere with respect to the beam axis, and a polar angle of the sphericity axis between 40° and 140°. In addition the momentum imbalance had to be less than 20 GeV/c.

Hadrons coming from bottom quark fragmentation were selected with the help of the large impact parameter for the decay products of B-hadrons. Due to the long lifetime of B-hadrons and their large mass and high momentum, the computed probability P_E for all the decay products in the event to come from the primary interaction point is typically small. Requiring $P_E < 0.01$ selected a sample of 217,000 events with a purity of 83%. The technique used is described in detail in [10].

The same method was used to obtain a light quark sample: requiring $P_E > 0.5$ gave a sample of 357,000 events consisting of 79% light, 14% charm and 7% bottom quark events.

The c-quark fragmentation function was determined by a different method. Firstly, 2580 D^{*+} candidates were reconstructed in the channel $D^{*+} \to D^0\pi^+$ followed by $D^0 \to K^-\pi^+$ as described in [11]. Then an additional enrichment in charm quarks was achieved by requiring $0.005 < P_E < 0.015$, which reduced the background from D-mesons originating from B-meson decays. The resulting sample consisted of 50% c-quark, 18% light-quark, and 32% b-quark events. In the simulated data, charm events with D^* mesons showed the same momentum spectrum as all charm events. Thus there was no indication of bias due to the tagging. However, to be independent of any such bias, only the hemispheres opposite to the reconstructed D^* were used to measure the charged particle spectrum, weighting each particle by a factor of two.

Detector effects and the effects of selection cuts and impurities from other quark species have been corrected by computing correction factors

$$c_i = \frac{G_i}{M_i} \tag{5}$$

for each bin of each distribution from a detailed simulation of the detector after generating the hadronic Z^0 decays using the JETSET PS model [12]. Here G_i is the bin content of the generated distribution and M_i the corresponding bin content of the fully simulated Monte Carlo distribution. The corrected x distributions are plotted in Fig. 1 together with the corresponding simulated spectra. Since for the samples containing charm and bottom

events these factors were falling below 0.1 for $x > 0.8$, the corresponding x bins have been excluded from the fit. The systematic errors were estimated as max[0.03,0.1(1-c_i)]/c_i of the bin value, thus increasing the error for large correction factors. The resulting momentum distributions are tabulated in table 1.

The gluon fragmentation function was determined from tagged gluon jets in b-quark induced 3-jet events. Both bottom quark jets were tagged by requiring $P_j < 0.01$, where P_j differs from P_E only in referring to the tracks in a single jet, and the remaining jet was taken as a gluon jet if its value of P_j exceeded 0.1. A total of 6791 gluon jets were identified with a purity of 94%. For these gluon jets, the fraction of the jet momentum $x_j = p_h/p_{jet}$ of the charged particles in the jet was measured and was used in the fit described in the next section. This technique has been described in detail in [13], and the results have been taken from that analysis.

The systematic uncertainties were estimated by varying the selection criteria. Changing the minimum number of charged particles from 5 to 6 and varying the cut on the sphericity axis between 30° and 45° changed the correction factors by typically 3% in the intermediate x range used in the fit.

To extract the scaling violation, we used all flavour mix spectra from the following experiments:

- DELPHI 91 GeV [1]
- ALEPH 91 GeV [14,15]
- AMY 54 GeV [16]
- TASSO 44, 35, 22, 14 GeV [17]
- CELLO 35 GeV [1,18]
- MARK II 29 GeV [19]

A global fit has to take into account the correlations between the data points of a given spectrum, e.g. coming from a common normalization error. For those experiments where the normalization errors were absorbed in the total error, the following procedure was adopted. The total error $\sigma_{tot}^{(i)}$ was split into an experimental error $\sigma_{exp}^{(i)}$ for each data point i of a given spectrum and an assumed overall normalization error σ_n for all data points of that spectrum:

$$\sigma_{tot}^{(i)\,2} = \sigma_{exp}^{(i)\,2} + \sigma_n^2 \tag{6}$$

The experimental error for a given point was obtained by quadratically subtracting σ_n from the quoted total error. In order to avoid the experimental error squared becoming negative by this procedure, it was required to exceed a certain minimum value σ_{min}. The whole analysis was then repeated for various values of σ_{min} and the σ_n. The result found to be insensitive to these values, as expected since the main effect of the scaling violation is to change the shapes of the spectra, not their overall normalizations.

4 Determination of the strong coupling constant

The fragmentation functions defined in equation (4) cannot be derived in perturbative QCD. Only the energy evolution (equation (2)) is predicted. Therefore a parametrization of the fragmentation functions is needed at one energy, from which the evolution starts, and these parameters have to be the same at all other energies, so that the differences between the momentum spectra at different energies depend only on α_s.

In this analysis, the parametrization from Ref. [14] was used:

$$xD_i(x,Q_0) = N_i \; \frac{x^{a_i}(1-x)^{b_i} \;\; \exp(-c(\ln x)^2)}{\int_{0.1}^{0.8} \; dx \;\; x^{a_i}(1-x)^{b_i} \;\; \exp(-c(\ln x)^2)} \tag{7}$$

where the coefficients N_i, a_i and b_i were allowed to take different values for the spectra for light (uds) quarks, c-quarks, b-quarks and gluons (g); Q_0 is the "starting energy" which was taken to be 91.2 GeV. In addition to the uds, c, b and g spectra, the spectra summed over all quarks and gluons were also used. These '*total*' spectra are parametrized by a_t and b_t. Since a_t and b_t cannot be independent parameters, the parametrization for the spectra from the light quarks (uds) was obtained from the total spectra minus the spectra for b and c quarks. The exponential term in (7) is inspired by the Modified Leading-Log Approximation (MLLA) [20] which predicts

$$\frac{d\sigma}{d\ln x} \sim \exp(-c(\ln x)^2) \tag{8}$$

with a single value c for all quark flavours as well as for the gluon. The boundaries of the integral in (7) correspond to the x range used in the analysis: the fit was performed only in the range $0.1 \leq x \leq 0.8$, since for smaller x the parametrization failed to describe the data.

The experimental momentum distributions from DELPHI are displayed in Fig. 2 together with the corresponding parametrizations, as determined from the global fit. This was a simultaneous fit of the QCD scale $\Lambda^{(5)}_{\overline{MS}}$ and the fragmentation parameters a_i, N_i, b_i and c defined in (7), and was made by minimizing the following χ^2 function:

$$\chi^2 = \Delta^T V^{-1} \Delta. \tag{9}$$

Here Δ is a column vector containing the residuals between the content of a given x bin of the inclusive momentum spectrum for a given Q^2 and the theoretical prediction. The latter can be computed at any value of Q^2 by evolution of the spectra from the starting energy of 91 GeV; the reference spectra at 91 GeV were parametrized by equation 7; the evolution was done by numerical integration of equations (1) and (2) with the program discussed in [6]. The matrix V is the N by N covariance matrix between N measurements. The elements of V are defined as follows:

- the diagonal elements are given by the square of the total experimental errors;
- the off-diagonal elements of correlated points are given by the product of the errors common to them (the overall normalization error).

In the range $0.10 < x < 0.80$ and $14^2 < Q^2 < 91.2^2$ GeV^2, a total of 14 parameters including $\Lambda^{(5)}_{\overline{MS}}$ were fitted to the 13 distributions of the data from section 3. The renormalization scale μ_R^2 and the factorization scale μ_F^2 were set equal to Q^2. This resulted in $\Lambda^{(5)}_{\overline{MS}} = 318^{+109}_{-96}$ MeV, which corresponds to $\alpha_s(M_Z) = 0.126^{+0.006}_{-0.007}$.

The χ^2 per degree of freedom of the fit was 174.5/175 and the fit parameters are given in table 2. The x dependence for different Q^2 values and the Q^2 dependence for different x-bins are shown in Figs. 3 and 4 respectively, together with the best fits.

Alternatively, a different definition of χ^2 can be used in which the correlations between the data points are included using an overall normalization factor for each momentum spectrum of each experiment:

$$\chi^2 = \sum_j \left[\sum_i \left(\frac{(n_j D^{(i)} - T^{(i)})^2}{(n_j \sigma^{(i)}_{exp})^2} \right) + \frac{(1-n_j)^2}{\sigma_n^2} \right]. \tag{10}$$

Here n_j is the normalization factor for experiment j with data $D^{(i)}$ in a given x bin with an experimental error $\sigma_{exp}^{(i)}$ for that bin and an overall normalization error σ_n for that experiment. The different definitions of χ^2 can introduce different biases in the fit results, especially if the errors are dominated by systematic effects [21]. The maximum deviation from the central value of the previous fit corresponded to $\delta\alpha_s(M_Z) = 0.002$; so if there is any bias, it is small compared with the total error.

No dependence of α_s on the renormalization and factorization scales, μ_R and μ_F, is expected if all higher orders are known. In this analysis the leading logarithms have been resummed, so one expects a smaller scale dependence than in the previous analysis, which was done only up to $O(\alpha_s^2)$. However, the scale dependence of α_s does not decrease with respect to the $O(\alpha_s^2)$ result, as shown in Fig. 5. Furthermore, the different scales all describe the momentum spectra equally well, so there is no experimentally preferred scale. The theoretical error due to the renormalization and factorization scale uncertainty was estimated from the α_s variation in Fig. 5 for scale variations between $0.5\sqrt{s}$ and $2\sqrt{s}$ to be:

$$\delta\alpha_s(M_Z) = ^{+0.007}_{-0.010}\ (theory),$$

where the error is half the maximum variation.

Non-perturbative corrections might exist at the lower energies. This energy dependence would simulate a scaling violation. Possible non-perturbative effects have been tested by changing variables, i.e. by replacing x with $x = f(x')$, where x' is the measured quantity. Assuming that at the scale $\sqrt{s} = \sqrt{s_0}$ all non-perturbative effects are absorbed in the fragmentation functions, the relation between the perturbative value of x and the observed value x' can be parametrized by [6]:

$$x = x' + h_0 \left(\frac{1}{\sqrt{s}} - \frac{1}{\sqrt{s_0}} \right).$$

The fitted value of h_0 was -0.07 ± 0.11, which is compatible with zero, indicating that non-perturbative effects are small.

An additional check for non-perturbative corrections was carried out by changing the lowest Q^2 value in the fit between 14^2 and 29^2 GeV^2. This did not change the value of α_s outside the errors. The resulting maximum deviation was $\delta\alpha_s(M_Z) = \pm 0.002$.

Combining the theoretical errors in quadrature and symmetrizing them yields:

$$\alpha_s(M_Z) = 0.124^{+0.006}_{-0.007}(exp) \pm 0.009(theory).$$

The theory error is larger than that for the α_s determination in [1] using the string or independent fragmentation model, mainly because of the unexpectedly large error from the factorization and renormalization scale dependences. After resumming the leading logarithms, there is no reason to restrict these scales to be below the centre-of-mass energy, so all scales in the range $0.5\sqrt{s} < \mu < 2\sqrt{s}$ were considered. In our previous analysis using the complete matrix-element, one could calculate the jet cross-sections for each scale, and large scales were found not to describe the jet cross-sections. Consequently the upper limit on the scale was taken to be $\mu = \sqrt{s}$. In the present analysis using the DGLAP equations, no correspondence with the jet cross-sections is given and the momentum spectra themselves are equally well described by all scales, so one cannot reduce the range of scales.

The experimental errors are larger too, since the DGLAP evolution equations require a parametrization of the inclusive momentum spectra of the quarks (uds, c, and b) and gluons by arbitrary polynomials and exponentials, which is difficult for spectra varying

over more than 4 orders of magnitude with a non-trivial shape, so this requires many parameters. In our previous $O({\alpha_s}^2)$ analysis, the LUND and Peterson parametrizations of the fragmentation functions were used for the primary mesons. The complete spectra were obtained by adding the secondary mesons and gluon fragmentation for every event in the same way, and using the same hadron decay parameters for all events. With this additional knowledge about the fragmentation process one can describe the spectra better over a larger x range with fewer parameters, and this resulted in smaller experimental errors.

5 Summary

Scaling violation in the fragmentation functions of quarks from e^+e^- annihilation has been investigated using the DGLAP evolution equations in next-to-leading order. From the variation of the scaled momentum distributions with Q^2 in the range $14^2\mathrm{GeV}^2$ to $91^2\mathrm{GeV}^2$, the strong coupling constant was determined to be

$$\alpha_s(M_Z) = 0.124^{+0.006}_{-0.007}(exp) \pm 0.009(theory).$$

This value is in agreement with our previous determination of α_s from the scaling violation, $\alpha_s = 0.118 \pm 0.005$ [1], with the recently measured precise value from the Z^0 lineshape parameters, $\alpha_s = 0.121 \pm 0.003 \pm 0.002$ [4], and with a similar analysis of scaling violation by ALEPH, $\alpha_s = 0.126 \pm 0.009$ [15].

Our previous analysis of scaling violation used the exact second order QCD matrix element, implying different systematics and higher order corrections, as explained in the introduction. The errors in the present analysis are larger than in the previous analysis, mainly because of the more involved parametrization needed for the DGLAP equations and the larger scale dependence. Therefore the cross check with the previous analysis has limited precision, but within this precision the agreement is satisfactory.

Acknowledgments

We would like to thank B.R. Webber and P. Nason for useful discussions and providing programs for the numerical integration of the DGLAP equations.

References

[1] DELPHI Coll., P. Aarnio et al.: Phys. Lett. **B311** (1993) 408.

[2] The LEP Colls. (ALEPH, DELPHI, L3, OPAL), Phys. Lett. **B276** (1992) 247;
ALEPH Coll., D. Decamp et al., Phys. Lett. **B255** (1991) 623; ibid. **B257** (1991) 479;
DELPHI Coll., P. Abreu et al., Phys. Lett. **B247** (1990) 167; ibid. **B252** (1990) 159; Z. Phys. **C54** (1992) 55;
L3 Coll., B. Adeva et al., Phys. Lett. **B248** (1990) 464; ibid. **B271** (1991) 461; ibid. **B284** (1992) 471;
OPAL Coll., M.Z. Akrawy et al., Phys. Lett. **B235** (1990) 389; ibid. **B252** (1990) 159; Z. Phys. **C49** (1991) 375; P.D. Acton et al., Phys. Lett. **B276** (1992) 547.

[3] S. Bethke and J.E. Pilcher, Ann. Rev. Nucl. Part. Sci. **42** (1992) 251;
T. Hebbeker, Phys. Rep. **217** (1992) 69;
M. Schmelling, 'Measurement of the strong coupling constant and tests of the structure of QCD', Invited talk given at the XV International Conference on Physics in Collision, Cracow, Poland, June 1995, CERN-PPE/95-129.

[4] The LEP Colls., A. Blondel, Plenary talk at the 28th Int. Conf. on High Energy Physics, Warsaw, July 1996;
LEP Electroweak Working Group, LEPEWWG/96-02;
W. de Boer et al., hep-ph/9609209.

[5] Y.L. Dokshitzer, JETP **73** (1971) 1216;
V.N. Gribov and L.N. Lipatov, Sov. J. Nucl. Phys. **15** (1972) 78;
G. Altarelli and G. Parisi, Nucl. Phys. **B126** (1977) 298;
G. Altarelli, Phys. Rep. **81** (1982) 1.

[6] P. Nason and B.R. Webber, Nucl. Phys. **B421** (1994) 473.

[7] G. Curci, W. Furmanski, R. Petronzio, Nucl. Phys. **B175** (1980) 27.

[8] Review of Particle Properties, Phys. Rev. **D50** (1994).

[9] DELPHI Coll., P. Aarnio et al., Nucl. Instr. and Meth. **A 303** (1991) 233;
DELPHI Coll., P. Abreu et al., Nucl. Instr. and Meth. **A 378** (1996) 57.

[10] DELPHI Coll., P. Abreu et al., Z. Phys. **C65** (1995) 555;
G.V. Borisov and C. Mariotti, Nucl. Instr. and Meth. **A 372** (1996) 181;
G.V. Borisov, 'Lifetime Tag of events $Z^0 \longrightarrow b\bar{b}$ with the DELPHI detector', DELPHI 94-125 PROG 208.

[11] DELPHI Coll., 'Study of charm mesons production in Z^0 decays and measurement of Γ_c/Γ_h', EPS-HEP Conference, Brussels, July 1995, Ref. eps0557 and DELPHI 95-101 Brussels PHYS 536.

[12] T. Sjöstrand, Comp. Phys. Comm. **39** (1986) 347;
T. Sjöstrand and M. Bengtsson, Comp. Phys. Comm. **43** (1987) 367.

[13] DELPHI Coll., P. Abreu et al., Z. Phys. **C70** (1996) 179.

[14] ALEPH Coll., D. Buskulic et al., Z. Phys. **C55** (1992) 209.

[15] ALEPH Coll., D. Buskulic et al., Phys. Lett. **B357** (1995) 487.

[16] AMY Coll., Y.K. Li et al., Phys. Rev. **D41** (1990) 2675.

[17] TASSO Coll., W. Braunschweig et al., Z. Phys. **C47** (1990) 187.

[18] O. Podobrin, Ph.D. Thesis, Univ. of Hamburg, 1992, and private communication.

[19] MarkII Coll., A. Petersen et al., Phys. Rev. **D37** (1988) 1.

[20] C.P. Fong and B.R. Webber, Nucl. Phys. **B355** (1991) 54.

[21] G. D'Agostini, Nucl. Instr. and Meth. **A346** (1994) 306.

x range	$1/\sigma_{tot}\ d\sigma/dx$		
	b-quarks	c-quarks	uds-quarks
0.00 - 0.01	415±6±12	283±10±9	274.5±0.5±8.2
0.01 - 0.02	455±6±14	380±11±11	357.5±0.5±10.7
0.02 - 0.03	309±4±9	244±9±7	232.3±0.4±7.0
0.03 - 0.04	216±3±7	189±8±6	160.8±0.4±4.8
0.04 - 0.05	162±2±5	141±7±4	118.5±0.3±3.6
0.05 - 0.06	126.8±1.6±3.8	115±7±4	91.2 ±0.3±2.7
0.06 - 0.07	100.9±1.3±3.0	82±5±3	72.7 ±0.3±2.2
0.07 - 0.08	82.0±1.1±2.5	66±5±2	59.3 ±0.2±1.8
0.08 - 0.09	66.7±0.9±2.0	59±5±2	49.3 ±0.2±1.5
0.09 - 0.10	55.7±0.8±1.7	50±4±2	41.6 ±0.2±1.3
0.10 - 0.12	42.5±0.6±1.3	40.8±2.9±1.2	32.9±0.1±1.0
0.12 - 0.14	30.2±0.4±0.9	30.1±2.4±0.9	24.9±0.1±0.8
0.14 - 0.16	22.3±0.3±0.7	24.4±2.3±0.7	19.4±0.1±0.6
0.16 - 0.18	16.2±0.3±0.5	18.5±2.0±0.6	15.3±0.1±0.5
0.18 - 0.20	12.3±0.2±0.4	13.1±1.7±0.4	12.4±0.1±0.4
0.20 - 0.25	7.6±0.1±0.2	8.7±0.8±0.3	8.84±0.04±0.27
0.25 - 0.30	4.03±0.07±0.12	6.0±0.8±0.2	5.61±0.03±0.17
0.30 - 0.40	1.86±0.04±0.06	2.95±0.37±0.09	3.06±0.02±0.09
0.40 - 0.50	0.678±0.017±0.020	0.96±0.19±0.03	1.40±0.01±0.04
0.50 - 0.60	0.235±0.009±0.007	0.32±0.10±0.01	0.672±0.008±0.020
0.60 - 0.70	0.069±0.007±0.007	0.16±0.12±0.02	0.319±0.006±0.010
0.70 - 0.80	0.016±0.007±0.003	-	0.148±0.004±0.006
0.80 - 1.00	-	-	0.037±0.001±0.002

Table 1: Corrected inclusive momentum distribution $1/\sigma_{tot}\ d\sigma/dx$ for b, c and uds quarks, DELPHI. The data have been corrected for detector effects, backgrounds and selection cuts. The first error quoted is statistical, the second is systematic. Data points with x below 0.1 or above 0.8 were not used in the fit.

Parameter	Result	Error
a_t	-1.525	± 0.013
b_t	1.824	± 0.012
N_t	0.707	± 0.002
a_c	-1.280	± 0.047
b_c	2.833	± 0.115
N_c	0.371	± 0.006
a_b	-1.652	± 0.045
b_b	3.063	± 0.097
N_b	0.295	± 0.003
a_g	-1.281	± 0.020
b_g	3.829	± 0.075
N_g	0.369	± 0.002
c	0.236	± 0.003
$\Lambda^{(5)}_{\bar{M}S}$ (MeV)	318	$^{+109}_{-96}$

Table 2: Parameters of the fragmentation functions and their errors: The lower subscripts stand for t = total, i.e. for the parameters for the spectra from all events, c = c-quark, b = b-quark, g = gluon.

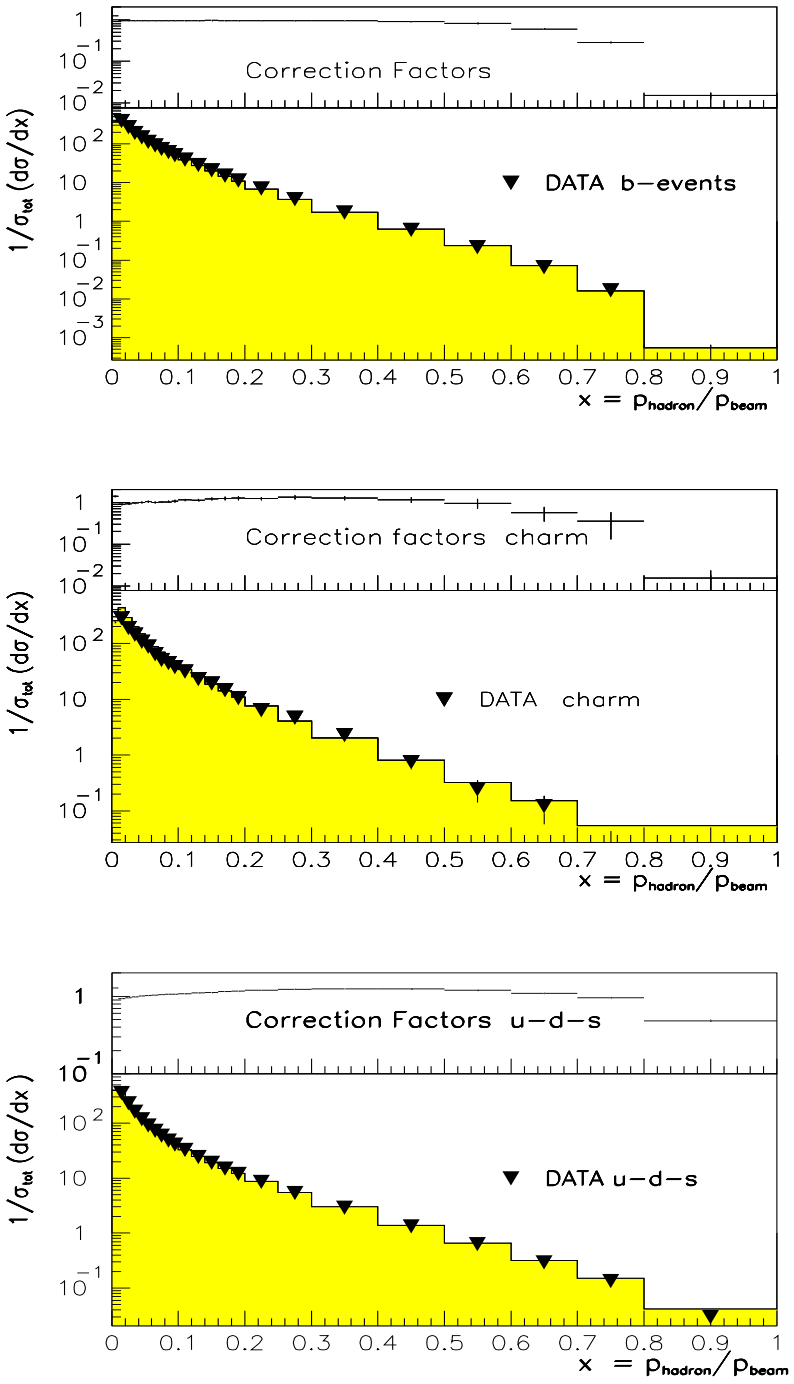

Figure 1: The corrected x distribution for bottom events (upper plot), charm events (middle plot), and light-quark events (lower plot) and the corresponding Monte Carlo distribution (shaded). The upper insets show the correction factors for detector effects, cuts and backgrounds (eq. 5).

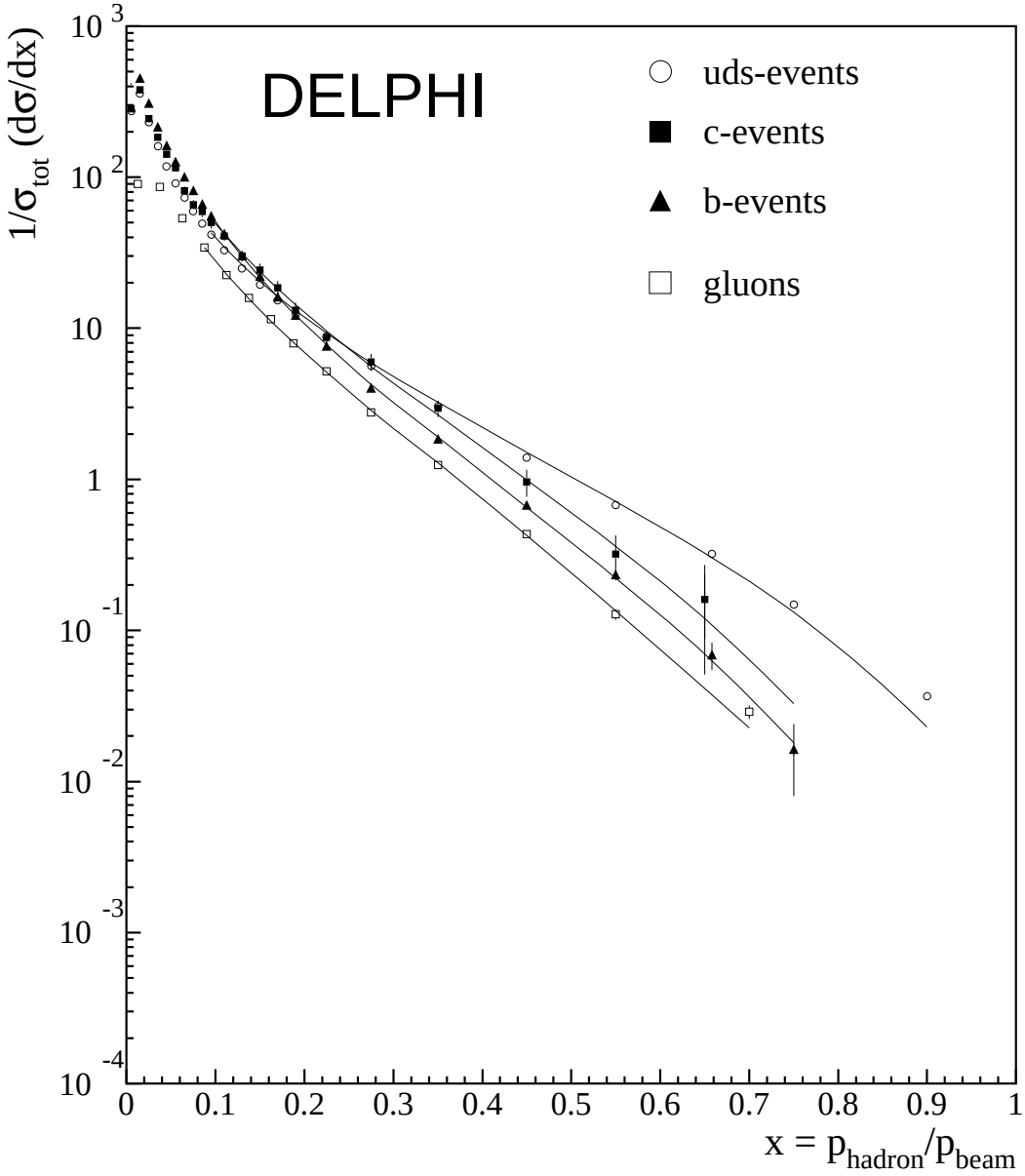

Figure 2: Flavour-specific scaled momentum distributions at 91 GeV. The curves are results of the fit in the region between 0.10 and 0.80. The gluon jets were tagged in 3-jet events with $x = p_{hadron}/p_{jet}$. The gluon distribution is lower mainly because of the lower multiplicity of a single jet compared to the complete events.

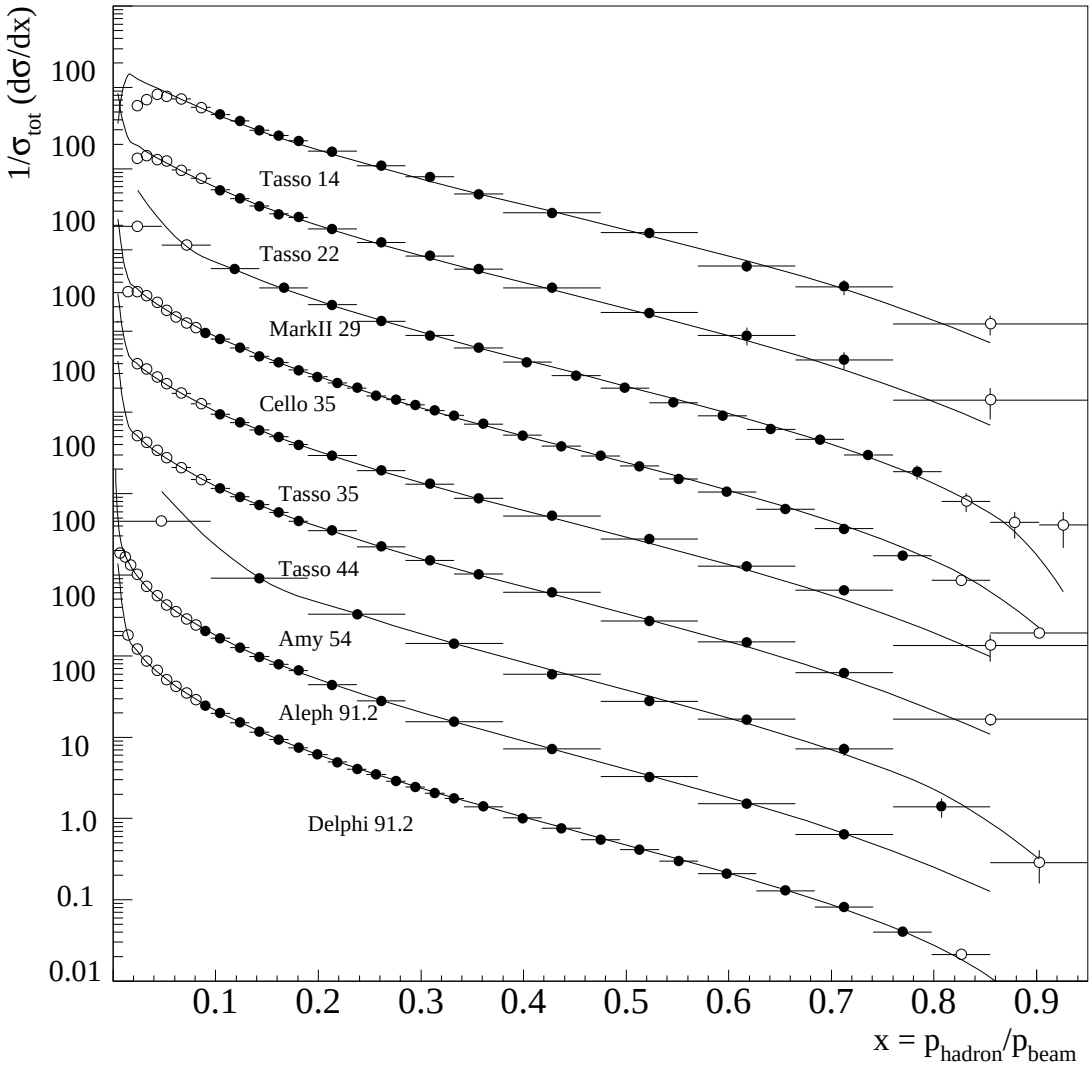

Figure 3: Inclusive scaled momentum distributions at centre-of-mass energies in the range between 14 GeV and 91.2 GeV. Only the full dots have been used in the fit.

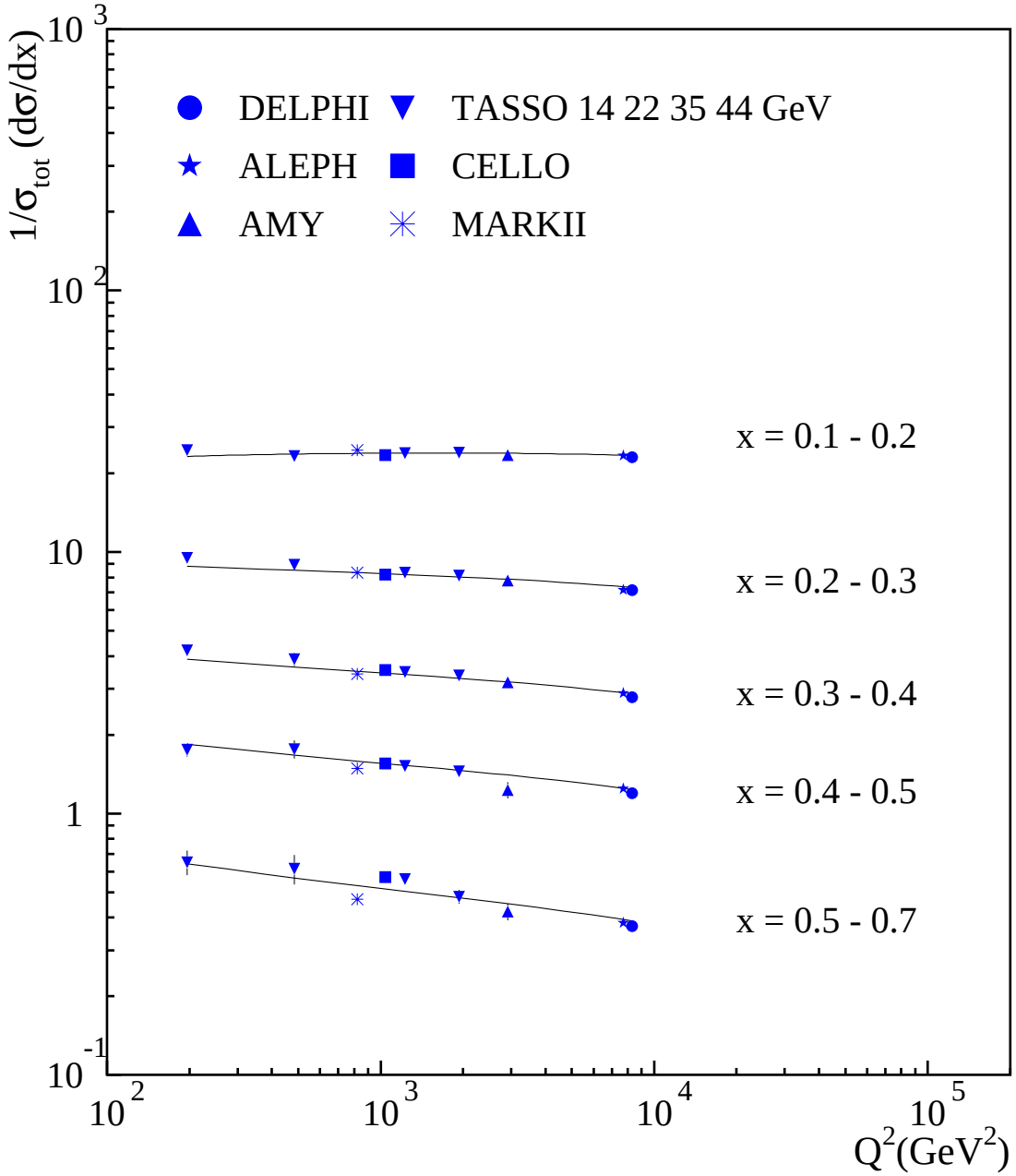

Figure 4: The Q^2 dependence of the inclusive momentum cross-section in GeV^2 for various x bins. For most data points the errors are smaller than the symbols. The curves are results of the fit for $0.10 < x < 0.70$.

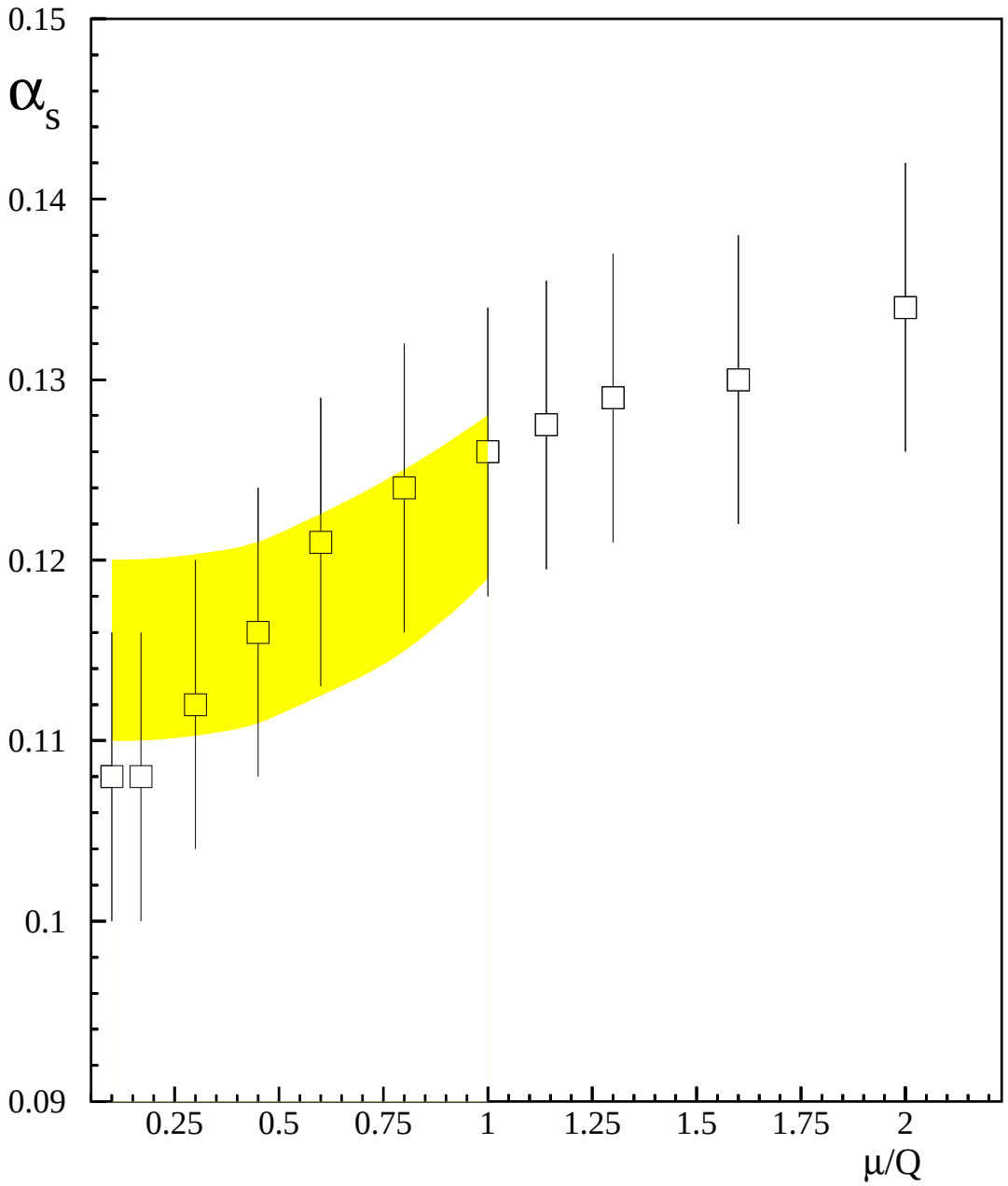

Figure 5: The renormalization and factorization scale dependence of α_s. The shaded area corresponds to the measurements based on the exact second order matrix element (from [1]).